

4.3. ELECTRON DIFFRACTION

$$\begin{aligned}
 I(s) &= I_a(s) + I_m(s) \\
 &= \frac{I_0}{R^2} \left\{ \sum_{i=1}^M [|f_i|^2 + |g_i|^2 + 4S_i(s)/(a^2 s^4)] \right. \\
 &\quad + \sum_i^M \sum_{j \neq i}^M [|f_i| |f_j| \cos(\eta_i^f - \eta_j^f) + |g_i| |g_j| \cos(\eta_i^g - \eta_j^g)] \\
 &\quad \left. \times \int_0^\infty dr P_{ij}(r, T)(\sin sr)/sr \right\}, \quad (4.3.3.3)
 \end{aligned}$$

where $|g_i|$ and η_i^g refer to the scattering-factor magnitude and phase for electrons that have changed their electron spin state during the scattering process and $|f_i|$ and η_i^f refer to retention of spin orientation. The incident electron beam is assumed to be unpolarized and no attempt has been made to consider relativistic effects on the inelastic scattering cross section, which is usually negligible in the structural s range.

If it is necessary to consider binding effects, the first Born approximation may usually be used in describing molecular scattering, since binding effects are largest for molecules containing small atoms where the Born approximation is most valid.

The exact expression for $I(s)$ in the first Born approximation can be written as (Bonham & Fink, 1974; Tavad & Roux, 1965; Tavad, Rouault & Roux, 1965; Iijima, Bonham & Ando, 1963; Bonham, 1967)

$$\begin{aligned}
 I(s) &= \frac{4I_0}{a^2 s^4 R^2} \left\{ \sum_{i=1}^M (Z_i^2 + Z_i) \right. \\
 &\quad + \sum_i^M \sum_{j \neq i}^M Z_i Z_j \int_0^\infty dr P_{ij}(r, T)(\sin sr)/sr \\
 &\quad - 2 \sum_{i=1}^M Z_i \left\langle \int dr \rho(r + r_i)(\sin sr)/sr \right\rangle_{\text{vib}} \\
 &\quad \left. + \left\langle \int dr \rho_c(r)(\sin sr)/sr \right\rangle_{\text{vib}} \right\},
 \end{aligned}$$

where

$$\rho(r) = \sum_{i=1}^N \int dr_1 \dots \int dr_N |\psi(r_1, \dots, r_N)|^2 \delta(r - r_i)$$

and

$$\rho_c(r) = \sum_i^N \sum_{j \neq i}^N \int dr_1 \dots \int dr_N |\psi(r_1, \dots, r_N)|^2 \delta(r - r_i + r_j).$$

The brackets $\langle \rangle_{\text{vib}}$ denote averaging over the vibrational motion, $\delta(r)$ is the Dirac delta function, and $\psi(r_1, \dots, r_n)$ is the molecular wavefunction. Binding effects appear to be proportional to the ratio of the number of electrons involved in binding to the total number of electrons in the system (Kohl & Bonham, 1967; Bonham & Iijima, 1965) so that binding effects in molecules containing mainly heavy atoms should be quite small.

The intensities, $I(s)$, for many small molecules have been calculated based on molecular Hartree–Fock wavefunctions. In most cases, a distinctive minimum has been found at about $s = 3 - 4 \text{ \AA}^{-1}$ and a much smaller maximum at $s = 8 - 10 \text{ \AA}^{-1}$ in the cross-sectional difference curve between the IAM and the molecular HF results (Pulay, Mawhorter, Kohl & Fink, 1983; Kohl & Bartell, 1969; Liu & Smith, 1977; Epstein & Stewart,

1977; Sasaki, Konaka, Iijima & Kimura, 1982; Shibata, Hirota, Kakuta & Muramatsu, 1980; Horota, Kakuta & Shibata, 1981; Xie, Fink & Kohl, 1984). Further studies using correlated wavefunctions (accounting for up to 60% of the correlation energy) showed that in the elastic channel the binding effects are only weakly modified; only the maximum at $s = 8 - 10 \text{ \AA}^{-1}$ is further reduced. However, strong effects are seen in the inelastic channel, deepening the minimum at $s = 3 - 4 \text{ \AA}^{-1}$ significantly (Breitenstein, Endesfelder, Meyer, Schweig & Zittlau, 1983; Breitenstein, Endesfelder, Meyer & Schweig, 1984; Breitenstein, Mawhorter, Meyer & Schweig, 1984; Wang, Tripathi & Smith, 1994). Detailed calculations on CO_2 and H_2O averaging over many internuclear distances and applying the pair distribution functions $P_{ij}(r)$ showed that vibrational effects do not alter the binding effects (Breitenstein, Mawhorter, Meyer & Schweig, 1986). For CO_2 , the calculations have been confirmed in essence by an experimental set of data (McClelland & Fink, 1985). However, more molecules and more detailed analysis will be available in the future. The binding effects make it desirable to avoid the small-angle-scattering range when structural information is the main goal of a diffraction analysis.

The problem of intramolecular multiple scattering may necessitate corrections to the molecular intensity when three or more closely spaced heavy atoms are present. This correction (Karle & Karle, 1950; Hoerni, 1956; Bunyan, 1963; Gjønnes, 1964; Bonham, 1965a, 1966) appears to be more serious for three atoms in a right triangular configuration than for a collinear arrangement of three atoms. A case study by Kohl & Arvedson (1980) on SF_6 showed the importance of multiple scattering. However, their approach is too cumbersome to be used in routine structure work. A very good approximate technique is available utilizing the Glauber approximation (Bartell & Miller, 1980; Bartell & Wong, 1972; Wong & Bartell, 1973; Bartell, 1975); Kohl's results are reproduced quite well using the atomic scattering factors only. Several applications of the multiple scattering routines showed that the internuclear distances are rather insensitive to this perturbation, but the mean amplitudes of vibration can easily change by 10% (Miller & Fink, 1981; Kelley & Fink, 1982a; Ketkar & Fink, 1985).

Acknowledgements

The authors acknowledge with gratitude the contributions of Kenneth and Lise Hedberg, who made many helpful suggestions regarding the manuscript and carefully checked the numerical results for smoothness and consistency.

 4.3.4. Electron energy-loss spectroscopy on solids
(By C. Colliex)

4.3.4.1. Definitions

4.3.4.1.1. Use of electron beams

Among the different spectroscopies available for investigating the electronic excitation spectrum of solids, inelastic electron scattering experiments are very useful because the range of accessible energy and momentum transfer is very large, as illustrated in Fig. 4.3.4.1 taken from Schnatterly (1979). Absorption measurements with photon beams follow the photon dispersion curve, because it is impossible to vary independently the energy and the momentum of a photon. In a scattering experiment, a quasi-parallel beam of monochromatic particles is incident on the specimen and one measures the changes in energy and momentum that can be attributed to the creation of a given excitation in the target. Inelastic neutron scattering is the most

4. PRODUCTION AND PROPERTIES OF RADIATIONS

powerful technique for the low-energy range ($\lesssim 0.1$ eV). On the other hand, inelastic X-ray scattering is well suited for the study of high momentum and large energy transfers because the energy resolution is limited to ~ 1 eV and the cross section increases with momentum transfer. In the intermediate range, inelastic electron scattering [or electron energy-loss spectroscopy (EELS)] is the most useful technique. For recent reviews on different aspects of the subject, the reader may consult the texts by Schnatterly (1979), Raether (1980), Colliex (1984), Egerton (1986), and Spence (1988).

4.3.4.1.2. Parameters involved in the description of a single inelastic scattering event

The importance of inelastic scattering as a function of energy and momentum transfer is governed by a double differential cross section:

$$\frac{d^2\sigma}{d\Omega d(\Delta E)}, \quad (4.3.4.1)$$

where $d\Omega$ corresponds to the solid angle of acceptance of the detector and $d(\Delta E)$ to the energy window transmitted by the spectrometer. The experimental conditions must therefore be defined before any interpretation of the data is possible. Integrations of the cross section over the relevant angular and energy-loss domains correspond to partial or total cross sections, depending on the feature measured. For instance, the total inelastic cross section (σ_i) corresponds to the probability of suffering any energy loss while being scattered into all solid angles. The discrimination between elastic and inelastic signal is generally defined by the energy resolution of the spectrometer, that is the minimum energy loss that can be unambiguously distinguished from the zero-loss peak; it is therefore very dependent on the instrumentation used.

The kinematics of a single inelastic event can be described as shown in Fig. 4.3.4.2. In contrast to the elastic case, there is no simple relation between the scattering angle θ and the transfer of momentum $\hbar\mathbf{q}$. One has also to take into account the energy loss ΔE . Combining both equations of conservation of momentum and energy,

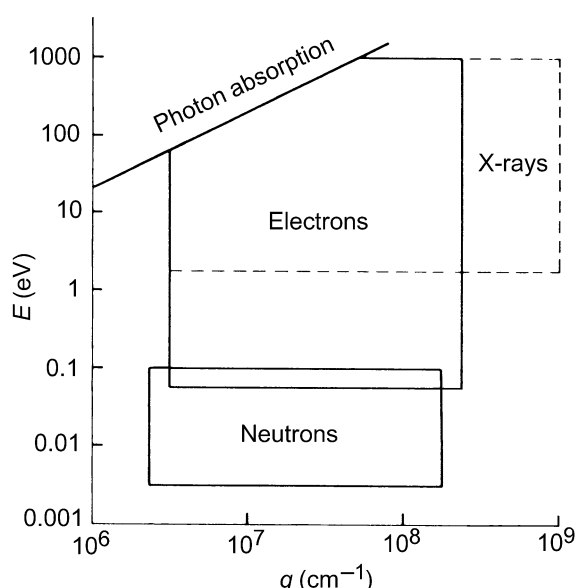


Fig. 4.3.4.1. Definition of the regions in (E, q) space that can be investigated with the different primary sources of particles available at present [courtesy of Schnatterly (1979)].

$$\frac{\hbar^2 k'^2}{2m_0} + \Delta E = \frac{\hbar^2 k^2}{2m_0}, \quad (4.3.4.2)$$

and

$$q^2 = k^2 + k'^2 - 2kk' \cos \theta, \quad (4.3.4.3)$$

one obtains

$$(qa_0)^2 = \frac{2E_0}{R} \left[1 - \left(1 - \frac{\Delta E}{E_0} \right)^{1/2} \cos \theta \right] - \frac{\Delta E}{R}, \quad (4.3.4.4)$$

where the fundamental units $a_0 = \hbar^2/m_0e^2 =$ Bohr radius and $R = m_0e^4/2\hbar^2 =$ Rydberg energy are used to introduce dimensionless quantities. In this kinematical description, one deals only with factors concerning the primary or the scattered particle, without considering specifically the information on the ejected electron. For a core-electron excitation of an atom, one distinguishes \mathbf{q} (the momentum exchanged by the incident particle) and χ (the momentum gained by the excited electron), the difference being absorbed by the recoil of the target nucleus (Maslen & Rossouw, 1983).

4.3.4.1.3. Problems associated with multiple scattering

The strong coupling potential between the primary electron and the solid target is responsible for the occurrence of multiple inelastic events (and of mixed inelastic-elastic events) for thick specimens. To describe the interaction of a primary particle with an assembly of randomly distributed scattering centres (with a density N per unit volume), a useful concept is the mean free path defined as

$$\Lambda = 1/N\sigma \quad (4.3.4.5)$$

for the cross section σ . The ratio t/Λ measures the probability of occurrence of the event associated with the cross section σ when the incident particle travels a given length t through the material. This is true in the single scattering case, that is when $t/\Lambda \ll 1$.

For increased thicknesses, one must take into account all multiple scattering events and this contribution begins to be non-negligible for $t \gtrsim$ a few tens of nanometres. Multiple scattering is responsible for a broadening of the angular distribution of the

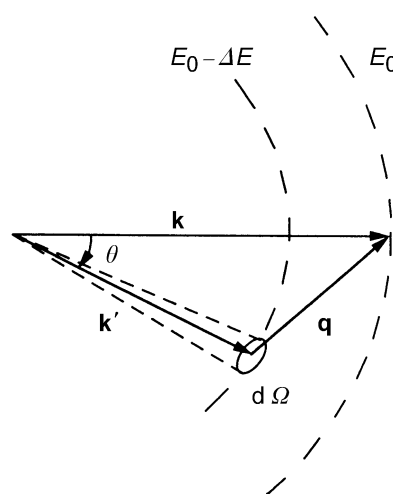


Fig. 4.3.4.2. A primary electron of energy E_0 and wavevector \mathbf{k} is inelastically scattered into a state of energy $E_0 - \Delta E$ and wavevector \mathbf{k}' . The energy loss is ΔE and the momentum change is $\hbar\mathbf{q}$. The scattering angle is θ and the scattered electron is collected within an aperture of solid angle $d\Omega$.